Nickel complexes of a bis(benzimidazolin-2-ylidene)pyridine pincer ligand with four- and five-coordinate geometries

David H. Brown,[*,a,b] and Brian W. Skelton[c]

[a] Nanochemistry Research Institute, Department of Chemistry, Curtin University, GPO Box U1987, Perth WA 6845, Australia

[b] School of Biomedical, Biomolecular and Chemical Sciences, The University of Western Australia, 35 Stirling Hwy, Crawley, WA 6009, Australia

[c] Centre for Microscopy, Characterisation and Analysis, The University of Western Australia, 35 Stirling Highway, Crawley, WA 6009, Australia.

[*] To whom correspondence should be addressed. E-mail: d.h.brown@curtin.edu.au. Tel: +61 8 9266 1279. Fax: +61 8 9266 4699.

Abstract

The four- and five-coordinate complexes [(CNC)NiX$_2$] (X = Cl, Br, I), [(CNC)NiX]PF$_6$ (X = Cl, Br) and [(CNC)NiCl]Cl·H$_2$O have been isolated, where CNC is the bis(N-butylbenzimidazolin-2-ylidene)-2,6-pyridine pincer ligand. A five-coordinate geometry is rare for this class of complex. Where amenable, the complexes have been structurally characterised by single crystal X-ray diffraction studies and in solution by NMR, UV-vis and MS studies. The five-coordinate dibromo complex [(CNC)NiBr$_2$] is readily prepared on the gram-scale from the benzimidazolium salt precursor and Ni(OAc)$_2$·4H$_2$O in DMSO without the exclusion of air. Halide exchange and salt metathesis reactions using [(CNC)NiBr$_2$] afford the other four- and five-coordinate complexes. [(CNC)NiBr$_2$] displays very low solubility, and upon dissolution affords solutions of the four-coordinate [(CNC)NiBr]$^+$. Factors that influence the formation of four- or five-coordinate complexes with this ligand class are discussed.

Introduction

Within the diverse field of *N*-heterocyclic carbene metal complexes,[1] ligand systems involving a 'pincer' binding geometry with a range of donor groups have been extensively studied.[2,3,4] As a subset, CNC 'pincer' ligands based on pyridine with pendant NHC donors (*e.g.* ligand in **1**) have been explored with considerable depth.[2,3] In particular, the imidazole-derived ligands, bis(imidazolin-2-ylidene)-2,6-pyridine (*e.g.* ligand in **1**), which were first reported in 2000,[5] have since been used to form metal complexes with almost all of the *3d*, *4d* and *5d* d-block metals and a number of f-block metals.[2] These metal complexes have been explored for a range of reasons, including their catalytic activity,[2,3] luminescence[6] and electrochemical properties.[7]

|						
1	M = Pd	X = Br		**4**	M = Pd	X = Br
2	M = Pd	X = I		**5**	M = Pd	X = Cl
3	M = Ni	X = Br		**6**	M = Ni	X = Br
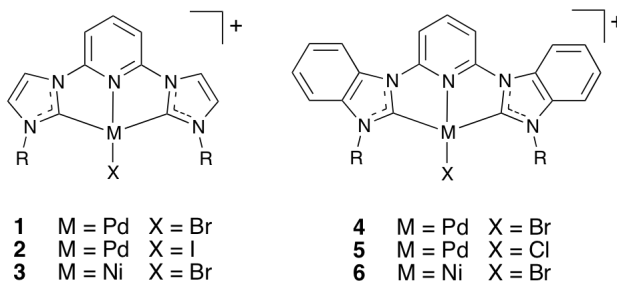
In comparison with the wide-spread investigation of the bis(imidazolin-2-ylidene)-2,6-pyridine ligand system, the analogous benzimidazole-based CNC pincer ligand, bis(benzimidazolin-2-ylidene)-2,6-pyridine (*e.g.* ligand in **4**), has been relatively unexplored. In 2008, Dötz, Tu and co-workers reported the first example of a complex with this ligand type, the palladium complex **4·Br** (R = Bu).[8] Since this report, a small number of complexes have been reported, including Pd,[9-11] Ag,[10] Os[7] and recently Ni ('**6·Br**' R = Bu).[12] The complexes have been investigated for their gelation (Pd),[9] catalytic (Pd and Ni),[8,11,12] electrochemical (Os)[7] and NHC-transfer properties (Ag).[10] It is somewhat surprising that the Pd and Ni complexes, in particular, have only recently been reported given the interest in the Pd[13,14,15] and Ni[16-18] complexes of the imidazole-based ligand bis(imidazolin-2-ylidene)-2,6-pyridine. However, even in the more general field of NHC metal complexes the use

of benzimidazolin-2-ylidines as ligands is, in general, considerably less advanced than that of the imidazolin-2-ylidines.

In this paper we report the synthesis and characterisation of a range of four- and five-coordinate complexes of the type [(CNC)NiX$_2$] and [(CNC)NiX]$^+$ bearing a bis(benzimidazolin-2-ylidene)-2,6-pyridine ligand. The complexes have been characterised in the solution and solid states, using ^{1}H and ^{13}C NMR, UV-vis and single crystal X-ray diffraction studies. A number of factors appear to influence the preference for particular systems to form either the four- or five-cooridnate complexes, and discussion is provided in this regard.

Results and Discussion

The reaction of the bis(benzimidazolium) dibromide salt **7**·2Br[10] with nickel acetate tetrahydrate in DMSO at 160°C for *ca*. 5 minutes, without the exclusion of air, afforded the five-coordinate [(CNC)NiBr$_2$] complex **8** in high yield (71%) as a dark purple microcrystalline material (Scheme 1) (see also ESI). This procedure is readily applied to the gram-scale syntheses of **8**. Our initial attempts to prepare the nickel complex used longer reaction times (*ca*. 1 h), at 140 °C, with precautions to exclude air, however it was discovered that such precautions and long reaction times were not needed. The procedure described here appears relatively facile, possibly a consequence of the geometry of the benzimidazole-based pincer ligand. Previously reported procedures for the synthesis of NHC-nickel(II) complexes are varied, but included: heating mixtures of azolium salts and nickel acetate under vacuum;[19,20] the addition of tetrabutylammonium bromide when using nickel acetate;[16,19] free-carbene methods;[21] and silver-transfer methods.[17,21] During this study, Tu et al. reported the complex **6**·Br (R = Bu).[12] However, based on their description of the complex, primarily its colour in the solid-state, we believe the complex they prepared was **8** (see our discussion below), though our studies suggest that dissolution of the complex would afford **6**·Br. No solid-state characterisation of the complex was previously reported.

3

7·2X X= Br or I

140 °C
or
160 °C

Ni(OAc)$_2$·4H$_2$O
DMSO
air

**8** X = Br 71%
9 X = I 65%
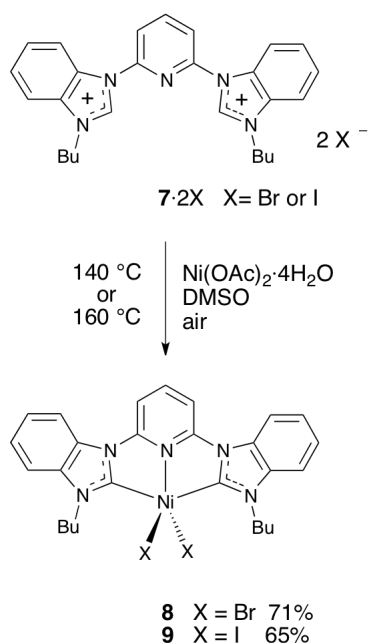
Scheme 1

The characterisation, and determination of the five-coordinate structure of **8** proved challenging. The solid-state appearance of the complex, as a dark purple solid, was significantly different from what was expected. The previously reported imidazolin-2-ylidene nickel bromide [(CNC)NiBr]Br complex **3·Br**, was described as a yellow-brown solid and the four-coordinate geometry of **3** was confirmed by a single-crystal X-ray diffraction study.[16] Complex **8** exhibited low solubility in a range of neat solvents including DMSO, water and acetonitrile. The complex was sparingly soluble in methanol (less than 0.5 mg/mL), affording yellow solutions. Extremely fine dark purple/black crystals were grown from methanol. A single-crystal X-ray diffraction study on the crystals revealed the dark purple complex **8** to have a five-coordinate trigonal bipyramidal geometry (see Solid-state studies). Due to the low solubility of the complex, an NMR study of the material proved difficult. Interestingly, in mixed solvent systems the complex was more soluble than the pure solvent alone. Dissolution of **8** in methanol-acetonitrile, methanol-water, acetonitrile-water and DMSO-water afforded yellow solutions, in which the complex remained dissolved. An increase in

the moisture content of 'pure' solvents appears to improve the solubility of **8** in the 'neat' solvent.

Heating a mixture of **8** in methanol afforded a yellow solution, though on cooling to room temperature dark purple/black needles rapidly precipitated leaving only a pale yellow solution. The dissolution of the dark purple [(CNC)NiBr$_2$] complex **8** in methanol to afford a pale yellow solution suggested that during the dissolution process the coordination geometry of the nickel centre was changing, possibly to a four-coordinate salt, similar to that of the yellow-brown imidazolin-2-ylidene [(CNC)NiBr]Br complex **3**·Br.[16] Salt metathesis of the bromide counter-anion in a complex of the type [(CNC)NiBr]Br with a non-coordinating anion could "trap" the four-coordinate complex, possibly in solution and the solid-state.

The treatment of a suspension of [(CNC)NiBr$_2$] complex **8** in hot methanol with potassium hexafluorophosphate results in a rapid change in the reaction mixture from a dark suspension to a bright orange solution. The addition of water to the solution affords the four-coordinate [(CNC)NiBr]$^+$ complex **10** as the hexafluorophosphate salt in high yield, as a bright orange powder (Scheme 2) (see also ESI). The salt **10**·PF$_6$ readily dissolves in methanol, acetonitrile, dichloromethane and chloroform, affording bright orange solutions. Very fine orange crystals of **10**·PF$_6$, which were suitable for a single crystal X-ray diffraction study, were grown from dichloromethane and diethyl ether solutions. The solid-state structure confirmed the four-coordinate square planar geometry (see Solid-state studies). ^{1}H NMR spectra of solutions of **10**·PF$_6$ in DMSO-d_6 or CDCl$_3$ often displayed broadened signals. However, ^{1}H NMR spectra of solutions of **10**·PF$_6$ in CD$_2$Cl$_2$ displayed sharp signals which were consistent with the proposed structure. The ^{13}C NMR spectrum of solutions of **10**·PF$_6$ in CD$_2$Cl$_2$ displayed a sharp signal at δ 170.4, which is attributed to the carbene carbon bound to nickel.
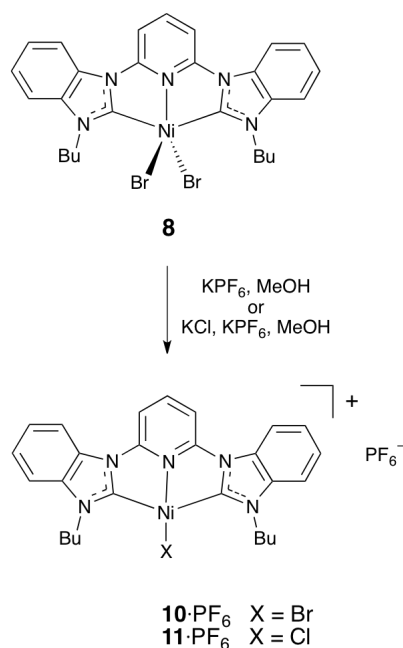
Scheme 2

Comparison of the UV-vis spectra for solutions of **8** and **10·PF$_6$** in methanol (Figure 1) indicated that the major absorption bands are very similar, including the bands at *ca*. 390-440 nm which are presumably due to d-d-transitions. This suggests that in both solutions the dissolved complex species have similar, if not identical, coordination geometries, presumably being the four-coordinate cation [(CNC)NiBr]$^+$ **10**. The dissolution of the dark purple complex [(CNC)NiBr$_2$] **8** in methanol to afford the yellow complex cation [(CNC)NiBr]$^+$ **10** suggests that there is an equilibrium between **8** and **10·Br** and that in methanol the formation of **10·Br** is 'favoured'. This equilibrium is supported by the observations that **8** is more soluble in methanol-water solutions than neat methanol, as the water would better solvate the bromide ion better than methanol, favouring the formation of **10·Br**. Likewise, in the preparation of **10·PF$_6$** the addition of potassium hexafluorophosphate to the methanol solution results in the rapid dissolution of **8**. In this case potassium bromide presumably precipitates from methanol, driving the dissolution, the equilibrium, and the formation of the cation **10**.
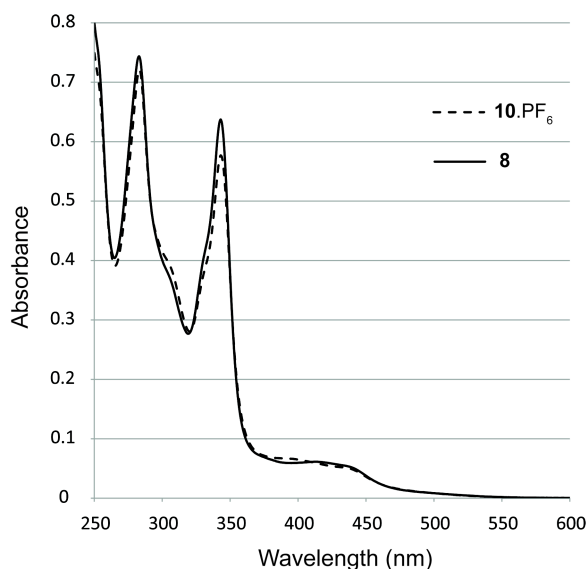
Figure 1. UV-vis spectra for solutions of **8** and **10**·PF$_6$ in methanol at *ca*. 2.5 x10^{-5} M

The reaction of the iodide salt **7**·2I with nickel acetate tetrahydrate in DMSO also afforded a dark purple powder, presumably complex **9,** analogous to that of the bromide system (Scheme 1). However, the iodo complex **9** displayed even lower solubility behaviour than **8**. The extremely low solubility of **9** in any solvent or solvent mixtures, prevented the solution characterisation of the complex, and all attempts to isolate a four-coordinate iodo complex using a similar procedure as described above for the conversion of **8** into **10**·PF$_6$ failed. The extremely low solubility of **9** presumably limits the reactivity, however, the size of the iodo ligand may also have a bearing on the stability of any four-coordinate complex (see Solid-state studies for more discussion).

An equilibrium between the four- and five-coordinate complexes **10** and **8** suggests that the addition of other halides to a solution of either complex may result in halide exchange reactions and formation of different nickel-halido complexes. The addition of a large excess of potassium chloride to a suspension of [(CNC)NiBr$_2$] complex **8** in hot methanol resulted in a rapid change in the reaction mixture from a dark suspension to a bright yellow solution. Subsequent addition of potassium hexafluorophosphate and then water afforded the four-coordinate [(CNC)NiCl]$^+$ complex **11** as the hexafluorophosphate salt in high yield, as a bright yellow powder (Scheme 2) (see also

ESI). As with the bromide analogue $10 \cdot PF_6$, the salt $11 \cdot PF_6$ was very soluble in methanol, acetonitrile, dichloromethane and chloroform. Very fine yellow crystals of $11 \cdot PF_6$, which were suitable for a single crystal X-ray diffraction study, were grown from dichloromethane and diethyl ether solutions. The solid-state structure confirmed the four-coordinate square planar geometry (see Solid-state studies). The ^{13}C NMR spectrum of solutions of $11 \cdot PF_6$ in CD_2Cl_2 displayed a sharp signal at δ 169.8, attributed to the carbene carbons bound to the nickel centre.

Using the above halide exchange procedure to prepare complexes of types $[(CNC)NiCl_2]$ or $[(CNC)NiCl]Cl$ was difficult. Treatment of a suspension of $[(CNC)NiBr_2]$ complex **8** in methanol with a large excess of potassium chloride resulted in yellow solutions, from which yellow powders could be isolated, however, they were invariably contaminated with residual bromide species. This contamination problem was resolved by using the anion exchange resin DOWEX® in the chloride form (DOWEX®-Cl). The treatment of the $[(CNC)NiBr_2]$ complex **8** in methanol with DOWEX®-Cl resulted in dissolution of the dark suspension and formation of a yellow solution (with suspended DOWEX® resin). The solution was then eluted through a column of DOWEX®-Cl with methanol. After evaporation of the filtrate, dissolution of the residue in ethanol and water and subsequent precipitation using a petroleum ether/diethyl ether solution, a wet yellow powder was isolated. The yellow powder was presumably the hydrated salt $[(CNC)NiCl]Cl \cdot xH_2O$ ($11 \cdot Cl \cdot xH_2O$) (see below). The material readily dissolves in methanol and ethanol. The ^1H NMR spectrum of a solution of $11 \cdot Cl \cdot xH_2O$ in CD_3OD displayed sharp signals that were consistent with the proposed structure, and the ^{13}C NMR spectrum of the same solution displayed a sharp signal at δ 170.2 (C-Ni). Interestingly, when yellow solutions of $11 \cdot Cl \cdot xH_2O$ in ethanol were concentrated to dryness, the residue sometimes appeared a dark purple colour. Dissolution of this dark coloured residue in ethanol would afford a bright yellow solution. Crystallisation experiments involving the dissolution of $11 \cdot Cl \cdot xH_2O$ in ethanol and then subsequent diffusion of vapours between the solution and THF afforded small black crystals (Note: The visual determination of crystal colour for small crystals

proved difficult. The crystals may be 'black' or dark purple.). When the solution of **11**·Cl·xH$_2$O in ethanol was more concentrated, then yellow crystals would sometimes initially form but with only black crystals being isolated on standing. Dissolution of the black crystals in alcoholic solutions affords yellow solutions. The black crystals were identified as the dichloro five-coordinate [(CNC)NiCl$_2$] complex **12**, with a trigonal bipyramidal geometry, by a single-crystal X-ray diffraction study (See Solid-state studies). In contrast, crystallisation attempts involving the dissolution of **11**·Cl·xH$_2$O in aqueous ethanol (*ca*. 5% water) and then subsequent diffusion of vapours between the solution and diethyl ether afforded yellow needles, that were determined to be the four-coordinate complex salt hydrate [(CNC)NiCl]Cl·3H$_2$O (**11**·Cl·3H$_2$O), with a square planar geometry around the nickel centre (See Solid-state studies). The solid-state structure shows that chloride anions are probably hydrogen bonded to water molecules in the crystal lattice. The behaviour described above is consistent with the equilibrium shown in Scheme 3, where the equilibrium position (*i.e*. the preference for **11** or **12**) depends on the solvation of chloride in solution or the solid state. In aqueous and alcoholic solutions, chloride is readily solvated, favouring the formation of **11**, but when water and solvent is removed then the formation of the five-coordinate **12** is favoured.
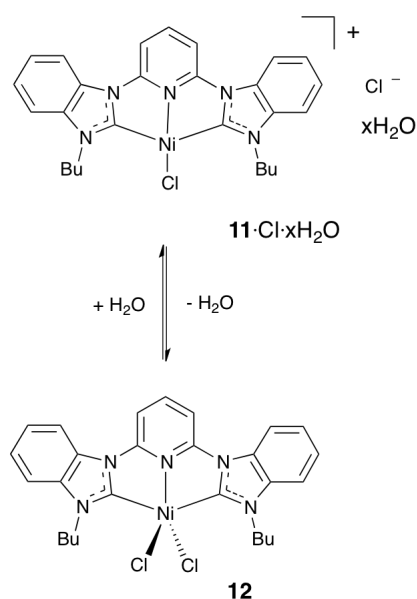
Scheme 3

The sharpness of the ^{1}H NMR spectra for the solutions of **10·PF$_6$** and **11·PF$_6$** in CD$_2$Cl$_2$ and **11·Cl** in CD$_3$OD are consistent with the complexes being diamagnetic, which is expected for four-coordinate square planar nickel(II) complexes. To determine the magnetic nature of the five-coordinate complex **8**, the magnetic moment of the complex was measured by a magnetic susceptibility balance, from which the complex was determined to also be diamagnetic.

Solid-state studies

All attempts to grow crystals of **8** afforded extremely fine needles of low quality. Not surprisingly, the data obtained from an X-ray diffraction study was not adequate for a satisfactory structure determination. However, it was possible to determine that in the solid-state, **8** has a five-coordinate approximately trigonal bipyrimidal geometry around the nickel centre.

Much more satisfactory results were obtained from the structure determination for the complexes **10·PF$_6$·CH$_2$Cl$_2$**, **11·PF$_6$**, **11·Cl·3H$_2$O** and **12**, even though all complexes also crystallised as fine needles. Crystal/refinement data is presented in Table 1, with selected bond lengths and angles for the complexes presented in Table 2.

In the structure of **10·PF$_6$**, the metal centre has an approximate square planar metal coordination environment (Figure 2). The coordination around the Ni atom in **10** differs significantly from planarity with the Br atom 0.528(4) Å out of the NC$_2$Ni plane (Figure 3). This deviation from planarity is also reflected in the N(21)-Ni(1)-Br(1) angle of 166.68(9)°, significantly different from 180°. The cation in **11·PF$_6$**, is similar to that of **10** in **10·PF$_6$**, monomeric with an approximate square planar metal coordination environment (Figure 4). Apart from the Ni-X bond lengths there are no other significant differences in the bond lengths and angles. As seen in **10·PF$_6$**, the coordinating atoms around the Ni atom in **11·PF$_6$** differs significantly from planarity with the Cl

atom 0.365(3) Å out of the NC$_2$Ni plane, and an N(21)-Ni(1)-Cl(1) angle of 170.68(6)° (Figure 5). In the case of **11,** the deviation of the Cl out of the NC$_2$Ni plane is less than that seen with the Br in **10**, presumably a consequence of chloride being smaller than bromide, resulting in a better 'fit' of the chloro ligand within the 'cavity' between the alkyl substituents on the benzimidazolyl ring.
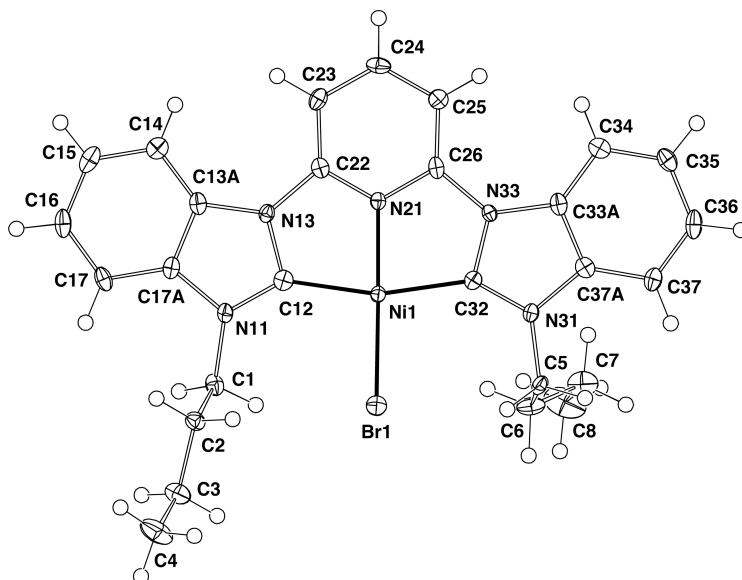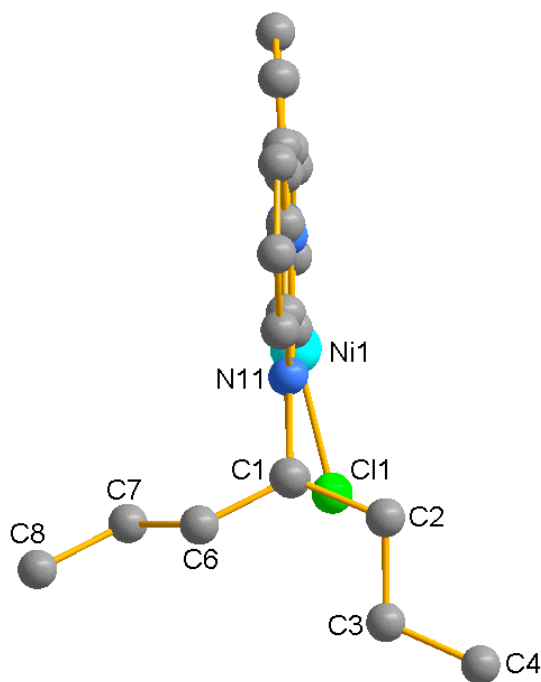

Figure 2. Molecular structure of the cation of **10**·PF$_6$·CH$_2$Cl$_2$, with displacement ellipsoids drawn at the 50% probability level.
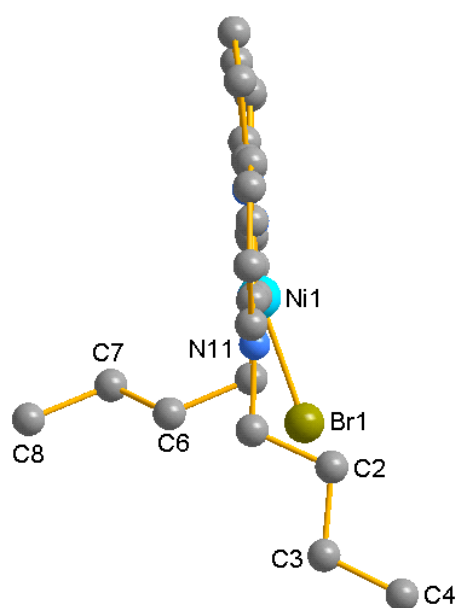
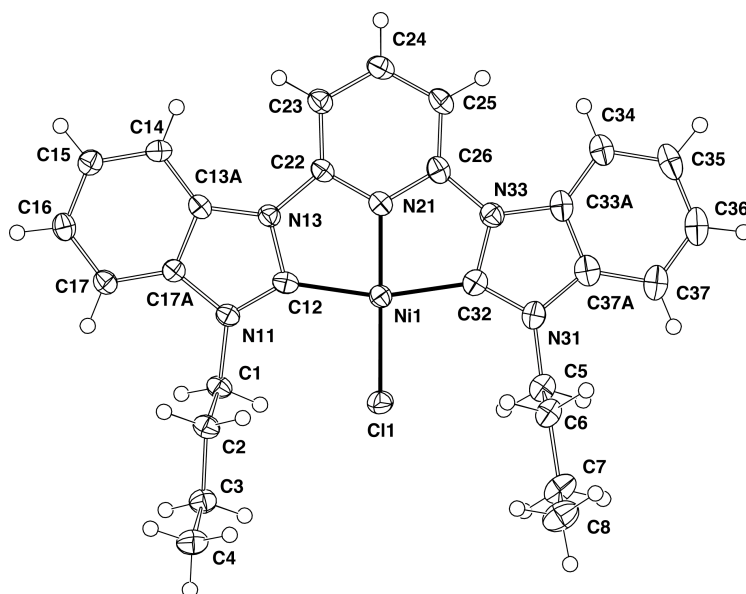**Figure 3**. 'Side-on' projection of the cation of **10**·PF$_6$·CH$_2$Cl$_2$
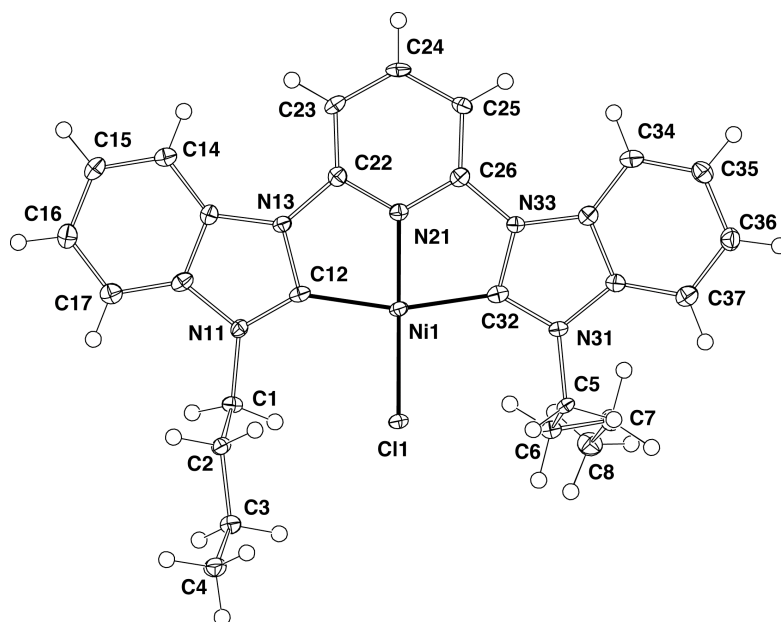
Figure 4. Molecular structure of the cation of **11**·PF$_6$, with displacement ellipsoids drawn at the

50% probability level.

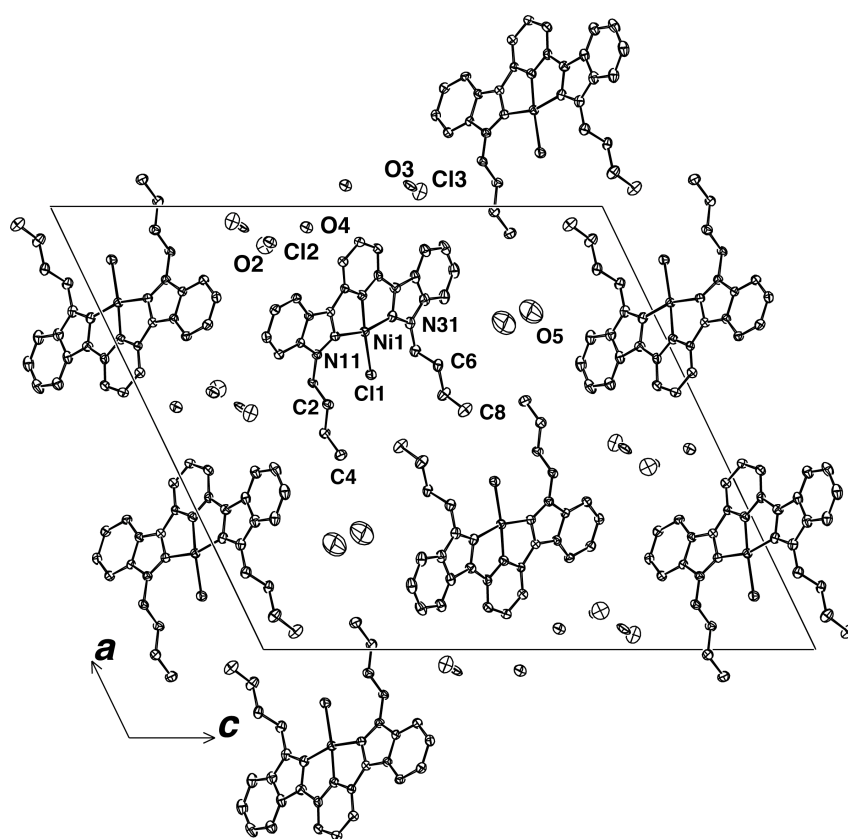**Figure 5**. 'Side-on' projection of the cation of **11**·PF$_6$

The cation of **11**·Cl·3H$_2$O is similar to that of the hexafluorophosphate salt **11**·PF$_6$, with an

approximate square planar metal coordination environment and a similar geometry except that the coordinated Cl is now more in the coordination plane, N(21)-Ni-Cl(1) 173.13(10) *cf.* 170.68(6) for **11**·PF$_6$ (Figure 6). Also, the nBu chains for **11** in **11**·Cl·3H$_2$O are *syn* relative to the coordination plane *cf.* the *anti* conformation for the cation in the PF$_6$ salt. Centrosymmetric pairs of cations are packed in the unit cell in a tail-to-tail and head-to-head fashion forming sheets about $z = 0,1$ and $z = 0.5$ with the planes of the molecules approximately parallel to the (0,1,4) and (0,-1,4) planes. This is shown in the cell plot (Figure 7). The angle between the planes of the molecules between adjacent sheets containing the cations is 82.2°. As a result of the short *b* axis, successive cations in this direction are sufficiently close for π-π interactions. The projection of the cation at x,1+y,z on the one at x,y,z is shown in Figure 8. Some close contacts are: C16...N11' 3.422(6), C22...N33' 3.425(5), C23...N33' 3.421(6), C23...O4' 3.225(6), C25...C34' 3.382(6), N33...C37' 3.363(6) Å where the prime refers to the atom in the molecule at x,1+y,z. From Figure 7, it can be seen that between the sheets of cations are columns of water molecules and chloride ions parallel to the *b* axis. There are two such columns, one consisting only of the water molecule O5, and the other of water molecules O3 and O4, and the chloride ions Cl2 and Cl3. Although these atoms are within distances expected for hydrogen bonding, as a result of the disorder in the latter column and since hydrogen atoms were not located for any of these water molecules, the geometric hydrogen bonding details are uncertain.

Figure 6. Structure of the cation of **11**·Cl·3H$_2$O, with displacement ellipsoids drawn at the 50% probability level.

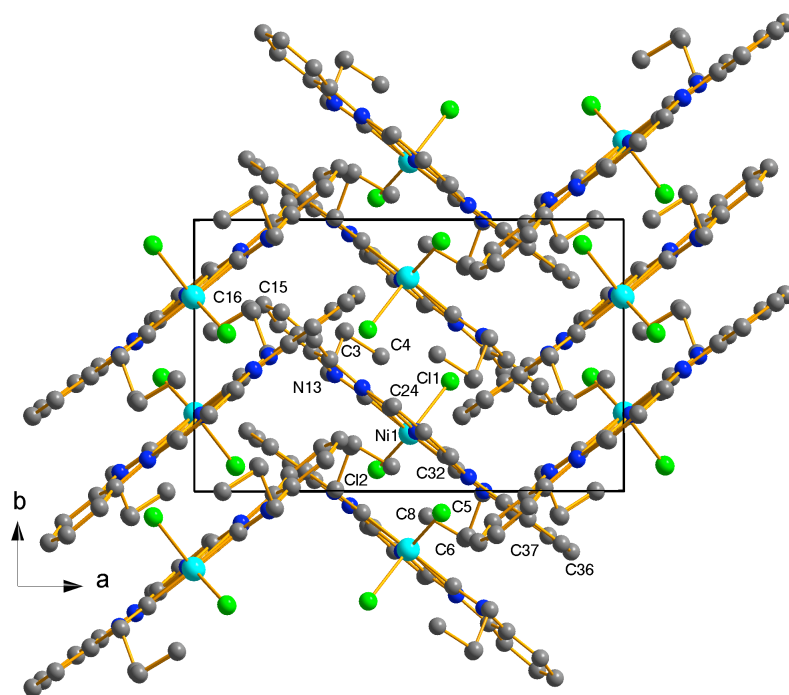**Figure 7**. Unit cell contents for **11**·Cl·3H$_2$O.
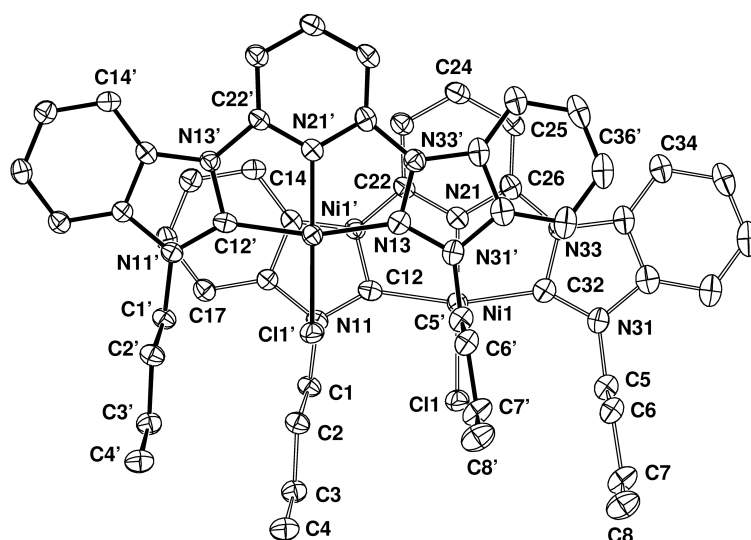
Figure 8. Projection of the cation of **11**·Cl·3H$_2$O at (x,1+y,z) (with black bonds) onto the one at (x,y,z). The primes refers to the atoms in the molecule at x,1+y,z. Hydrogen atoms have been omitted for clarity. Displacement ellipsoids have been drawn at the 50% probability level.

The structure for **12** is isomorphous with the bromo analogue **8** which was of low precision due to the small size of the crystals. The coordination environment in **12** approximates to trigonal bipyramidal, the two chloro atoms and N(21) forming the horizontal plane with C(12) and C(32) occupying the axial sites (Figure 9). The molecule possesses pseudo 2-fold symmetry with the n-butyl chains situated on either side of the coordination plane (see Figure 10). The ligand is essentially planar, the angles between the plane of the three rings being 4.7(2)° (ring 1/ring 2), 7.3(2)° (1/3), and 5.3(2)°(2/3). Pairs of centrosymmetric molecules form stacks approximately parallel to the (3,2,0) plane (see Figure 11) the distances between such sheets are 3.33 (between the molecule at x,y,z and that at 1-x,1-y,1-z) and 3.42Å (between the molecule at x,y,z and that at 1-x,-y,1-z). These stacks are then arranged in a herring-bone fashion in the unit cell (Figure 11). The coordination geometry of **12** is similar to that of [(CNC)PdI$_2$] complex **13**, which also adopts the five-coordinate trigonal bipyramidal geometry.

15

Figure 9. Molecular structure of the molecule **12** projected approximately on to the co-ordination plane, with displacement ellipsoids drawn at the 50% probability level.

Figure 10. Molecular structure of the molecule of **12** projected oblique to the coordination plane

Figure 11. Unit cell contents of **12** projected along the *c* axis. Hydrogen atoms have been omitted for clarity.

13
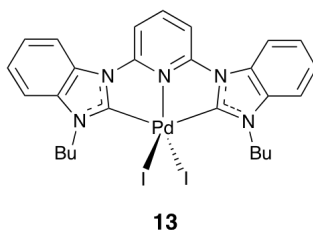
The coordination geometries of **8**, **12**, and the previously reported **13**[9] are somewhat unusual. The majority of the literature complexes of group 10 metals with CNC pincer ligands, of the type discussed here display a four-coordinate square planar geometry. The change in coordination geometry results in some significant changes. Apart from the obvious colour change there is also an unexpected significant difference in solubility. A comparison of the structures reported here with related complexes, containing either the imidazole- or benzimidazole-based NHCs and either nickel or palladium, suggests factors that may favour a five-coordinate geometry over a four-coordinate

geometry (Table 2). It would appear that one of the major factors may be the ease with which the halo ligand may 'fit' into the 'cavity' between the alkyl substituents on the NHC rings, as this position is what would be expected for an idealised square planar geometry in these complexes. Comparing the nickel complexes **10** and **11**, the increased size of bromide verses chloride results in a bigger deviation of the bromo ligand in **10** from the idealised square planar geometry. Presumably steric factors of the alkyl substituent force the halo ligands out of the idealised square planar geometry. The change from nickel to palladium (**11** versus **5**[10]) results in a complex where the chloro ligand can be accommodated into a square planar environment with little deviation from idealised geometries. Here the increase in the metal size from Ni to Pd forces the benzimidazolin-2-ylidene rings apart, widening the distance between the alkyl substituents. As a result steric interactions between the alkyl substitutents and the halo ligand are decreased. There is no reported example of a four-coordinate iodo analogue of **5**, only the five-coordinate complex **13**.[9] Presumably, even though the cavity size between the alkyl substituents is increased by the presence of palladium, iodide is too large to 'fit' into the available cavity, and as a result the five-coordinate complex is favoured, as the iodo ligands are now positioned in 'free space' above and below the plane of the pincer ligand. Our own attempts to synthesis an iodo analogue of the four-coordinate nickel complexes **10** and **11** were unsuccessful (see above), possibly for the same reason.

To date five-coordinate complexes complexes of group 10 metals with NHC-based CNC pincer ligands, of the type discussed here, have only been observed with benzimidazolin-2-ylidene ligands. The imidazolin-2-ylidene analogues have only been reported as four-coordinate complexes. The bromopalladium complex **1** (R=Bu) and the bromonickel complex **3** (R=Me) both display square planar geometries with only minor deviations of the halo ligand out of the idealised geometry [N-M-Br 177° for **1** (R=Bu)[14] and 176° for **3** (R=Me)[16]]. The difference between the imidazolin-2-ylidene and benzimidazolin-2-ylidene systems is a result of the differing geometries of the five-membered azole rings. The C=C bonds in imidazole rings are shorter than the analogous 'C=C'

bonds in benzimidazole rings. A consequence of this is that the angle that subtends the orientations of the *N*-substituents on imidazole rings is larger than that of analogous benzimidazole systems. In the case of the CNC pincer ligands discussed here, the alkyl substituents in the imidazole-based derivatives are splayed further apart than in their benzimidazole analogues. As a result, the 'cavity' between the alkyl substituents in the imidazole analogues is larger and thus the complexes readily form four-coordinate geometries (see R···R distances in Table 2).

Conclusion

We have reported the facile preparation of an unusual five-coordinate $[(CNC)NiBr_2]$ complex, bearing a benzimidazolin-2-ylidene-pyridine pincer ligand, that can be readily prepared on multi gram scales without the exclusion of air or moisture. Using a combination of salt metathesis and halide exchange reactions the complex is readily converted into four-coordinate complexes of the type $[(CNC)NiBr]PF_6$ and $[(CNC)NiCl]PF_6$. The different coordination geometries appear to have a significant influence on complex properties, particularly solubility. The five-coordinate $[(CNC)NiBr_2]$ complex displays solubility that is much lower than what would be expected. In addition, dissolution of the complex affords the four-coordinate $[(CNC)NiBr]^+$ in solution. Solvation of the bromide counter anion appears to have significant influence on the apparent 'solubility' of $[(CNC)NiBr_2]$. The chloro complex $[(CNC)NiCl_2]$ was also isolated, and depending on recrystallisation procedures (primarily based on water content of the solvent system) can be isolated as the five-coordinate $[(CNC)NiCl_2]$ or the four-coordinate $[(CNC)NiCl]Cl \cdot x H_2O$. The formation of four- or five-coordinate group 10 metal complexes with this, and the related imidazolin-2-ylidene, ligand system appears dependant on the size of cavity that is available between the substituents on the azol-2-ylidene rings. This cavity size can be affected by the azolin-2-ylidene ring type (imidazole vs benzimidazole) and the size of the metal, as well as presumably substituent type. For systems with smaller cavity sizes (Ni instead of Pd, and benzimidazole instead

of imidazole) the larger halido ligands favour the formation of five-coordinate geometries.

Experimental

General Methods. Nuclear magnetic resonance spectra were recorded using Varian Gemini 200 (200 MHz for ^{1}H, 50 MHz for ^{13}C) and Bruker Avance 500 (500.1 MHz for ^{1}H, 125.8 MHz for ^{13}C) spectrometers at ambient temperature. [1]H and ^{13}C chemical shifts were referenced to residual solvent resonances. Microanalyses were performed by the Central Science Laboratory at the University of Tasmania. UV-vis data was collected on a PerkinElmer LAMBDA 35 UV/VIS spectrometer. Magnetic moment measurements were made using a MSB-1 Magnetic Susceptibility Balance. Mass spectra were obtained by Dr A. Reeder (The University of Western Australia) using a VG Autospec Mass Spectrometer *via* fast atom bombardment (FAB) with a cesium ion source and a *m*-nitrobenzyl alcohol matrix. The benzimidazolium bromide salt **7·2Br** and 1,3-bis(benzimidazol-1-yl)pyridine were prepared by literature procedures.[10]

Benzimidazolium iodide   7·2I. A mixture of 1,3-bis(benzimidazol-1-yl)pyridine (1.44 g, 4.6 mmol) and 1-iodobutane (10 mL, 87 mmol) in DMF (20 mL) was heated at 100 °C for 24 h. The mixture was cooled and diluted with diethyl ether (50 mL). The resulting precipitate was collected, washed with diethyl ether (20 mL) and dried *in vacuo* to afford a colourless powder (3.1 g, 98%). (Found: C, 47.77; H, 4.65; N, 10.22. Calc. for $C_{27}H_{31}N_5I_2$: C, 47.73; H, 4.60; N, 10.31%); δ_H(200 MHz; DMSO-d_6) 0.99 (6 H, t, J = 7 Hz, 2 × CH_3), 1.48 (4 H, m, 2 × CH_2CH_3), 2.05 (4 H, m, 2 × NCH$_2$CH_2), 4.68 (4 H, t, J = 7 Hz, 2 × NCH$_2$), 7.69–7.87 (4 H, m, 4 × benzimidazolyl Ar CH), 8.30 (2 H, d, $J_{3,4}$ = 8 Hz, 2 × pyridyl H3), 8.34 (2 H, d, J = 8 Hz, 2 × benzimidazolyl Ar CH), 8.47 (2 H, d, J = 8 Hz, 2 × benzimidazolyl Ar CH), 8.78 (1 H, t, $J_{3,4}$ = 8 Hz, pyridyl H4), 10.70 (s, 1H, NCHN); δ_C(50 MHz; DMSO-d_6) 13.3 (CH$_3$), 19.0 (CH_2CH_3), 30.3 (NCH$_2CH_2$), 47.2 (NCH$_2$), 114.2 (CH), 115.6 (CH), 117.9 (CH), 127.3 (CH), 127.8 (CH), 129.5 (C), 131.5 (C), 142.6 (CH), 144.3 (CH), 146.3 (C).

[(CNC)NiBr$_2$] 8. A mixture of **7**·2Br (2.14 g, 3.7 mmol) and Ni(OAc)$_2$·4H$_2$O (1.1 g, 4.4 mmol) in DMSO (20 mL), under a normal laboratory atmosphere, was heated from RT to 160 °C and then held at 160 °C for *ca*. 5 min. The mixture was then allowed to cool to RT. The precipitate was collected, washed with ethanol (60 mL) and then air-dried. The solid was suspended in methanol (100 mL) and the mixture was heated at reflux for 24 h. The mixture was allowed to cool and the solid was collected, washed with methanol (40 mL) and dried *in vacuo* to afford a dark purple powder (1.7 g, 71%). (Found: C, 50.43; H, 4.70; N, 10.79. Calc. for C$_{27}$H$_{29}$N$_5$NiBr$_2$: C, 50.51; H, 4.55; N, 10.91%); HRMS (FAB+): *m/z* = 560.0978 (M-Br, C$_{27}$H$_{29}$N$_5$^{58}Ni^{79}Br requires 560.0960), 562.0967 (M-Br, C$_{27}$H$_{29}$N$_5$^{58}Ni^{81}Br requires 562.0939).

[(CNC)NiI$_2$] 9. A mixture of **7**·2I (377 mg, 0.56 mmol) and Ni(OAc)$_2$·4H$_2$O (180 mg, 0.72 mmol) in DMSO (5 mL) was heated at 140 °C for *ca*. 1 h. The mixture was then allowed to cool to RT. The precipitate was collected, washed with ethanol (40 mL), water (10 mL), ethanol (10 mL) and diethyl ether (10 mL) and then dried *in vacuo* to afford a dark purple powder (267 mg, 65%). (Found: C, 43.06; H, 4.14; N, 9.13. Calc. for C$_{27}$H$_{29}$N$_5$NiBr$_2$: Calc. for C$_{27}$H$_{29}$N$_5$NiI$_2$·H$_2$O: C, 43.01; H, 4.14; N, 9.29%); HRMS (FAB+): *m/z* = 608.0785 (M-I, C$_{27}$H$_{29}$N$_5$^{58}Ni^{127}I requires 608.0821).

[(CNC)NiBr]PF$_6$ 10·PF$_6$. A mixture of **8** (245 mg, 0.38 mmol) and KPF$_6$ (1.5 g, 8 mmol) in methanol (40 mL) was heated at reflux for 20 min. Water (40 mL) was added and the heating was continued for 5 min. The mixture was allowed to cool and the precipitate was collected, washed with water (40 mL) and dried *in vacuo* to afford an orange powder (251 mg). The powder was recrystallised by the diffusion of vapours between a solution of the material in dichloromethane and a solution of diethyl ether, to afford long orange needles (250 mg, 93%). (Found: C, 45.98; H, 3.96; N, 9.79. Calc. for C$_{27}$H$_{29}$N$_5$NiBrPF$_6$: C, 45.86; H, 4.13; N, 9.90%); δ_H(500 MHz; CD$_2$Cl$_2$) 1.04 (6 H, t, *J* = 7.4 Hz, 2 × CH$_3$), 1.57 (4 H, m, 2 × C*H$_2$*CH$_3$), 1.96 (4 H, m, 2 × NCH$_2$C*H$_2$*), 4.95 (4 H, t, *J* =

8.0 Hz, 2 × NCH$_2$), 7.60–7.73 (6 H, m, 6 × benzimidazolyl Ar CH), 7.85 (2 H, d, $J_{3,4}$ = 8.3 Hz, 2 × pyridyl H3), 8.03 (2 H, d, J = 8.2 Hz, 2 × benzimidazolyl Ar CH), 8.58 (1 H, t, $J_{3,4}$ = 8.3 Hz, pyridyl H4); δ_C(125 MHz; CD$_2$Cl$_2$) 13.9 (CH$_3$), 20.3 (CH$_2$CH$_3$), 32.7 (NCH$_2$CH$_2$), 47.7 (NCH$_2$), 108.4 (CH), 112.6 (CH), 113.1 (CH), 126.8 (CH), 127.6 (CH), 129.1 (C), 136.2 (C), 147.4 (CH), 151.8 (C), 170.4 (C-Ni). HRMS (FAB+): m/z = 560.0948 (M-PF$_6$, C$_{27}$H$_{29}$N$_5$^{58}Ni^{79}Br requires 560.0960), 562.0963 (M-PF$_6$, C$_{27}$H$_{29}$N$_5$^{58}Ni^{81}Br requires 562.0939). Crystals suitable for single crystal X-ray diffraction studies were grown by the diffusion of vapours between a solution of **10**·PF$_6$ in dichloromethane and a solution of diethyl ether.

[(CNC)NiCl]PF$_6$ 11·PF$_6$. A mixture of **8** (212 mg, 0.33 mmol) and KCl (1.6 g, 21 mmol) in methanol (40 mL) was heated at reflux for 20 min, during which time the mixture went from a dark purple mixture to a bright yellow-orange solution. To the solution was added KPF$_6$ (1.3 g, 7 mmol) and the mixture was heated for 5 min, then water (40 mL) was added and the mixture was heated for a further 2 min. The mixture was allowed to cool and the precipitate was collected, washed with water (40 mL) and dried *in vacuo* to afford a yellow powder (209 mg). The powder was recrystallised by the diffusion of vapours between a solution of the material in dichloromethane and a solution of diethyl ether, to afford long yellow needles (198 mg, 91%). (Found: C, 49.17; H, 4.48; N, 10.34. Calc. for C$_{27}$H$_{29}$N$_5$NiClPF$_6$: C, 48.94; H, 4.41; N, 10.57%); δ_H(200 MHz; CD$_2$Cl$_2$) 1.00 (6 H, t, J = 7 Hz, 2 × CH$_3$), 1.52 (4 H, m, 4H, 2 × CH_2CH$_3$), 1.93 (4 H, m, 2 × NCH$_2$CH_2), 4.85 (4 H, t, J = 8 Hz, 2 × NCH$_2$), 7.55–7.70 (6 H, m, 6 × benzimidazolyl Ar CH), 7.79 (2 H, d, $J_{3,4}$ = 8 Hz, 2 × pyridyl H3), 7.96-8.03 (2 H, m, 2 × benzimidazolyl Ar CH), 8.53 (1 H, t, $J_{3,4}$ = 8 Hz, pyridyl H4); δ_C(50 MHz; CD$_2$Cl$_2$) 14.3 (CH$_3$), 20.8 (CH$_2$CH$_3$), 33.1 (NCH$_2$CH$_2$), 47.2 (NCH$_2$), 108.8 (CH), 113.1 (CH), 114.5 (CH), 127.2 (CH), 128.0 (CH), 129.5 (C), 136.6 (C), 148.1 (CH), 152.4 (C), 169.8 (C-Ni); HRMS (FAB+): m/z = 516.1437 (M-PF$_6$, C$_{27}$H$_{29}$N$_5$^{58}Ni^{35}Cl requires 516.1465), 518.1382 (M-PF$_6$, C$_{27}$H$_{29}$N$_5$^{58}Ni^{37}Cl requires 518.1419). Crystals suitable for single crystal X-ray diffraction studies were grown by the diffusion of vapours between a solution of **11**·PF$_6$ in acetonitrile and a

solution of diethyl ether.

[(CNC)NiCl]Cl·*x*H₂O   11·Cl·*x*H₂O. A mixture of **8** (204 mg, 0.32 mmol) and DOWEX®-Cl (DOWEX® 1×8, 200-400 mesh, Cl⁻ form) in methanol (40 mL) was stirred for 3 h. The mixture was filtered, slowly, through a column of DOWEX-Cl®, and eluted with methanol. The yellow solution was concentrated *in vacuo* to afford a bright yellow solid. The solid was dissolved in ethanol (10 mL) and water (0.35 mL) and the result solution was diluted with a solution of petroleum ether (50 mL, b.p. fraction 60-80 °C) and diethyl ether (5 mL). The resulting precipitate was collected and dried to afford a bright yellow solid (203 mg). A sample was further dried *in vacuo* for microanalysis (Found: C, 54.95; H, 5.60; N, 11.62. Calc. for $C_{27}H_{29}N_5NiCl_2 \cdot 2H_2O$: C, 55.04; H, 5.65; N, 11.89%);δ_H(200 MHz, CD₃OD) 0.96 (6 H, t, J = 7 Hz, 2 × CH₃), 1.39 (4 H, m, 2 × CH_2CH₃), 1.81 (4 H, m, 2 × NCH₂CH_2), 4.58 (4 H, t, J = 8 Hz, 2 × NCH₂), 7.48–7.60 (4 H, m, 4 × benzimidazolyl Ar CH), 7.65-7.73 (2 H, m, 2 × benzimidazolyl Ar CH), 8.00 (2 H, d, $J_{3,4}$ = 8 Hz, 2 × pyridyl H3), 8.09-8.16 (2 H, m, 2 × benzimidazolyl Ar CH), 8.44 (1 H, t, $J_{3,4}$ = 8 Hz, pyridyl H4); δ_C(50 MHz, CD₃OD) 14.0 (CH₃), 20.9 (CH_2CH₃), 33.4 (NCH₂CH_2), 47.3 (NCH₂), 109.5 (CH), 113.6 (CH), 114.0 (CH), 127.5 (CH), 128.2 (CH), 129.8 (C), 136.9 (C), 148.1 (CH), 152.9 (C), 170.2 (C-Ni). Crystals suitable for single crystal X-ray diffraction studies were grown by the diffusion of vapours between a solution of **11**·Cl·*x*H₂O in ethanol (with *ca*. 5% water) and a solution of diethyl ether.

[(CNC)NiCl₂ 12. Dark purple/black crystals of **12** were grown by the diffusion of vapours between a solution of **11**·Cl·*x*H₂O in ethanol and a solution of thf. (Found: C, 58.82; H, 5.17; N, 12.57. Calcd for $C_{27}H_{29}N_5NiCl_2$: C, 58.63; H, 5.28; N, 12.66%).

X-ray Structure Determinations.

The crystal data for **10**·PF$_6$·CH$_2$Cl$_2$, **11**·PF$_6$, **11**·Cl·3H$_2$O and **12** are summarized in Table 1 with the structures depicted in various figures where ellipsoids have been drawn at the 50% probability level. Selected coordination geometries are shown in Table 2. Crystallographic data for the structures were collected at 100(2) K on an Oxford Diffraction Gemini diffractometer fitted with graphite-monochromated Mo Kα radiation (Cu Kα radiation for **11**·Cl·3H$_2$O and **12**). Following absorption corrections and solution by direct methods, the structures were refined against F^2 with full-matrix least-squares using the program SHELXL-97.[22] Except where specified, anisotropic displacement parameters were employed for all non-hydrogen atoms. Hydrogen atoms were added at calculated positions and refined by use of a riding model with isotropic displacement parameters based on the values of the parent atoms.

From the refinement of the solvent water molecules and chloride ions in **11**·Cl·3H$_2$O, it was apparent that the Cl$^-$ ion was disordered over two sites with water molecules. Site occupancy factors for the Cl$^-$ ion sites are 0.669(1) and 1-0.669(1). Water molecule hydrogen atoms were not located. The atoms of the minor component of one Cl/H$_2$O site were refined with isotropic displacement parameters.

References

1. F. E. Hahn and M. C. Jahnke, *Angew. Chem. Int. Ed.*, 2008, **47**, 3122-3172; A. T. Normand and K. J. Cavell, *Eur. J. Inorg. Chem.*, 2008, 2781-2800; S. Díez-González, N. Marion and S. P. Nolan, *Chem. Rev.*, 2009, **109**, 3612-3676.

2. M. Poyatos, J. A. Mata and E. Peris, *Chem. Rev.*, 2009, **109**, 3677-3707; D. Pugh and A. A. Danopoulos, *Coord. Chem. Rev.*, 2007, **251**, 610-641.

3. E. Peris and R. H. Crabtree, *Coord. Chem. Rev.*, 2004, **248**, 2239-2246.

4. D. Yuan, H. Tang, L. Xiao and H. V. Huynh, *Dalton Trans.*, 2011, DOI: 10.1039/c1dt10269a; H. V. Huynh, D. Yuan and Y. Han, *Dalton Trans.*, 2009, 7262-7268.

5. J. C. C. Chen and I. J. B. Lin, *J. Chem. Soc., Dalton Trans.*, 2000, 839-840.

6. C.-S. Lee, S. Sabiah, J.-C. Wang, W.-S. Hwang and I. J. B. Lin, *Organometallics*, 2010, **29**, 286-289; F. Jean-Baptiste dit Dominique, H. Gornitzka, A. Sournia-Saquet and C. Hemmert, *Dalton Trans.*, 2009, 340-352.

7. C. Y. Wong, L. M. Lai, P. K. Pat and L. H. Chung, *Organometallics*, 2010, **29**, 2533-2539.

8. T. Tu, J. Malineni and K. H. Dötz, *Adv. Synth. Catal.*, 2008, **350**, 1791-1795.

9. T. Tu, X. Bao, W. Assenmacher, H. Peterlik, J. Daniels and K. H. Dötz, *Chem. Eur. J*, 2009, **15**, 1853-1861.

10. D. H. Brown, G. L. Nealon, P. V. Simpson, B. W. Skelton and Z. Wang, *Organometallics*, 2009, **28**, 1965-1968.

11. T. Tu, X. Feng, Z. Wang and X. Liu, *Dalton Trans.*, 2010, **39**, 10598-10600.

12. T. Tu, H. Mao, C. Herbert, M. Z. Xu and K. H. Dötz, *Chem Commun*, 2010, **46**, 7796-7798.

13. E. Peris, J. A. Loch, J. Mata and R. H. Crabtree, *Chem. Commun.*, 2001, 201-202; A. A. D. Tulloch, A. A. Danopoulos, G. J. Tizzard, S. J. Coles, M. B. Hursthouse, R. S. Hay-Motherwell and W. B. Motherwell, *Chem. Commun.*, 2001, 1270-1271; P. G. Steel and C. W. T. Teasdale, *Tetrahedron Lett.*, 2004, **45**, 8977-8980; D. J. Nielsen, K. J. Cavell, B. W.

Skelton and A. H. White, *Inorg. Chim. Acta*, 2006, **359**, 1855-1869; F. Churruca, R. SanMartin, B. Inés, I. Tellitu and E. Domínguez, *Adv. Synth. Catal.*, 2006, **348**, 1836-1840; B. Inés, R. SanMartin, M. J. Moure and E. Domínguez, *Adv. Synth. Catal.*, 2009, **351**, 2124-2132; F. Godoy, C. Segarra, M. Poyatos and E. Peris, *Organometallics*, 2011, **30**, 684-688.

14. J. A. Loch, M. Albrecht, E. Peris, J. Mata, J. W. Faller and R. H. Crabtree, *Organometallics*, 2002, **21**, 700-706.

15. T. Tu, W. Assenmacher, H. Peterlik, R. Weisbarth, M. Nieger and K. H. Dötz, *Angew. Chem. Int. Ed.*, 2007, **46**, 6368-6371.

16. K. Inamoto, J.-i. Kuroda, K. Hiroya, Y. Noda, M. Watanabe and T. Sakamoto, *Organometallics*, 2006, **25**, 3095-3098.

17. K. Inamoto, J.-i. Kuroda, E. Kwon, K. Hiroya and T. Doi, *J. Organomet. Chem.*, 2009, **694**, 389-396.

18. K. Inamoto, J.-i. Kuroda, T. Sakamoto and K. Hiroya, *Synthesis*, 2007, 2853-2861; J.-i. Kuroda, K. Inamoto, K. Hiroya and T. Doi, *Eur. J. Org. Chem.*, 2009, 2251-2261; A. Mrutu, K. I. Goldberg and R. A. Kemp, *Inorg. Chim. Acta*, 2010, **364**, 115-119; A. Mrutu, D. A. Dickie, K. I. Goldberg and R. A. Kemp, *Inorg. Chem.*, 2011, **50**, 2729-2731.

19. H. V. Huynh, L. R. Wong and P. S. Ng, *Organometallics*, 2008, **27**, 2231-2237; H. V. Huynh, C. Holtgrewe, T. Pape, L. L. Koh and E. Hahn, *Organometallics*, 2006, **25**, 245-249; J. Berding, M. Lutz, A. L. Spek and E. Bouwman, *Organometallics*, 2009, **28**, 1845-1854.

20. H. V. Huynh and R. Jothibasu, *Eur. J. Inorg. Chem.*, 2009, 1926-1931.

21. D. Pugh, A. Boyle and A. A. Danopoulos, *Dalton Trans.*, 2008, 1087-1094.

22. G. M. Sheldrick, *Acta Crystallogr., Sect. A*, 2008, **64**, 112-122.

Table 1. Crystal data and refinement details for **10**·PF_6, **11**·PF_6, **11**·Cl·$3H_2O$ and **12**.

	10·PF_6·CH_2Cl_2	**11**·PF_6	**11**·Cl·$3H_2O$	**12**
Empirical formula	$C_{28}H_{31}BrCl_2F_6N_5NiP$	$C_{27}H_{29}ClF_6N_5NiP$	$C_{27}H_{35}Cl_2N_5NiO_3$	$C_{27}H_{29}Cl_2N_5Ni$
Formula weight	792.07	662.68	607.21	553.16
Crystal system	Triclinic	Triclinic	Monoclinic	Monoclinic
space group	$P\bar{1}$	$P\bar{1}$	$P2_1/n$	$P2_1/n$
a (Å)	7.4959(6)	8.8351(5)	23.7588(9)	13.7294(17)
b (Å)	10.4941(6)	9.5675(5)	4.9770(2)	8.6736(6)
c (Å)	20.1343(12)	15.9437(10)	26.5360(10)	20.423(3)
α (°)	85.314(5)	83.742(5)	90	90
β (°)	86.274(5)	87.414(5)	115.587(5)	92.463(10)
γ (°)	76.779(6)	82.567(5)	90	90
V (Å^3)	1534.94(18)	1327.77(13)	2830.09(22)	2429.8(5)
Z	2	2	4	4
D (Mg m^{-3})	1.714	1.658	1.425	1.512
μ (mm^{-1})	2.226	0.963	3.034	3.383
Transmission max/min	0.97/0.56	0.98/0.91	0.83/0.69	0.86/0.67
Crystal dimensions (mm)	0.74 x 0.05 x 0.014	0.38 x 0.03 x 0.02	0.45 x 0.10 x 0.06	0.24 x 0.08 x 0.04
θ_{max} (°)	28.64	32.56	67.21	67.29
Reflections collected	13531	15104	11979	25729
Unique reflections	6682	8661	4776	4314
R_{int}	0.051	0.0516	0.0329	0.0740
Reflections ($I>2\sigma(I)$)	4399	4838	3649	3240
Data/restraints/parameters	6682 / 0 / 399	8661 / 0 / 372	4776 / 0 / 360	4314 / 0 / 318
Goodness-of-fit	0.927	0.834	1.060	1.080
R_1, wR_2 [$I>2\sigma(I)$]	0.044, 0.095	0.0444, 0.0777	0.0536, 0.1613	0.0729, 0.2065
R_1, wR_2 [all data]	0.079, 0.101	0.1031, 0.0866	0.0716, 0.1749	0.0944, 0.2185
Largest peak, hole (e.Å^{-3})	0.66, -0.76	0.53, -0.45	1.35, -0.72	1.58, -0.53

Table 2. Selected Bond Distances (Å) and Angles (°) for **10**·PF$_6$·CH$_2$Cl$_2$, **11**·PF$_6$, **11**·Cl·3H$_2$O, and **12**, and compared against relevant examples from the literature.

Complex	M	X	azole	C-M (Å)	N-M (Å)	M-X (Å)	C-M-C (°)	N-M-X (°)	X-M-X (°)	R··Rᵃ (Å)	NC$_2$M···Xᵇ (Å)
[(CNC)MX]⁺											
10·PF$_6$·CH$_2$Cl$_2$	Ni	Br	benzimidazole	1.924(4), 1.932(4)	1.866(3)	2.2955(6)	163.08(14)	166.68(9)	-	6.547(6)	0.528(4)
11·PF$_6$	Ni	Cl	benzimidazole	1.911(2), 1.917(2)	1.8524(18)	2.1533(6)	162.90(9)	170.68(6)	-	6.382(4)	0.365(3)
11·Cl·3H$_2$O	Ni	Cl	benzimidazole	1.913(4), 1.922(4)	1.855(3)	2.1355(11)	163.43(16)	173.13(10)	-	6.476(6)	0.255(5)
5·BPh$_4$ R=Bu[10]	Pd	Cl	benzimidazole	2.0202(18), 2.0280(18)	1.9701(15)	2.2874(5)	158.94(7)	179.42(2)	-	6.777(3)	0.016(3)
3·Br R=Me[16]	Ni	Br	imidazole	1.921(5), 1.932(5)	1.862(4)	2.2783(8)	163.0(2)	176.4(1)	-	6.765(8)	0.144(5)
1·Br R=Bu[14]	Pd	Br	imidazole	2.017(13), 2.042(12)	1.957(10)	2.398(2)	158.66	177.2(3)	-	7.06(2)	0.11(3)
2·I R=Bu[15]	Pd	I	imidazole	2.044(3), 2.056(3)	1.984(2)	2.5736(3)	158.10(12)	174.22	-		
[(CNC)MX$_2$]											
12	Ni	Cl	benzimidazole	1.897(6), 1.900(7)	1.871(5)	2.2791(18), 2.4324(19)	162.0(3)	141.38(17), 115.64(17)	102.96(7)	6.270(10)	2.192(4), 1.424(6)
13 R=Bu[9]	Pd	I	benzimidazole								

ᵃ The distance between the two carbon atoms, of the alkyl substituents, bound to the azolyl nitrogen.

ᵇ The distance of the halide out of the NC$_2$M plane.

28